Progress of Theoretical Physics, Vol. 42, No. 3, September 1969

Alpha-Cluster plus ^{16}O-Core Model for ^{20}Ne and Neighboring Nuclei*)

Jun HIURA, Yasuhisa ABE, Sakae SAITŌ**) and Osamu ENDŌ***)

Department of Physics, Hokkaido University, Sapporo

(Received February 19, 1969)

A possibility of α-cluster structure in nuclei around ^{20}Ne is examined in terms of a model based on the assumption of *weak coupling* between an α cluster and an ^{16}O core. The model treats dynamically the coupling of α-^{16}O relative motion with a particle (p)- and a hole (h)-motion in an average nuclear field of ^{16}O. The $K^{\pi}=0^{+}$ rotational band of ^{20}Ne ($\alpha+^{16}$O) is plausibly explained with an effective α-^{16}O potential having repulsive core and state-dependent attractive well. The low-lying anomalous-parity levels of ^{19}F ($\alpha+^{16}$O$+h$) and the ground rotational band of ^{21}Ne ($\alpha+^{16}$O$+p$) are reasonably understood in terms of an effective nucleon-α potential with the essential features of the potential in free space. The hole and particle are treated in the weak- and strong-coupling schemes, respectively. The $K^{\pi}=2^{-}$ rotational band of ^{20}Ne* ($\alpha+^{16}$O$+p+h$) is well interpreted in the strong-coupling scheme for the p-h pair. In conclusion, certain successes of the model seem to suggest an importance of α-like four-body correlation or molecular aspect in light nuclei.

§ 1. Introduction

Many attempts have been made to explain various properties of light nuclei in terms of the shell model descriptions, namely the standard shell-model calculations,[2] the SU_3 model,[3] the method of deformed orbitals[4] and so on. These descriptions are essentially based on the average nuclear field and the two-body correlation.

However, another type of correlations, the so-called nucleon-clustering,[5] has also been considered to be an important concept in understanding the structure of some light nuclei. Several investigations based on the cluster model[6] and the α-particle model[7] have been carried out for the p-shell nuclei and have disclosed the existence of the α-clustering in nuclei.

The most stable nucleon-clustering in nuclei is expected to appear as an α-cluster, because of tightly bound internal structure of an α-particle and its weak interaction with a nucleon (N) or another α-particle. It is well established that the characteristic of the strong internal binding and the weak relative one is ascribed to the two-nucleon forces and to the Pauli principle.[8),9)] This fact makes it possible to represent N-α and α-α interactions in terms of effective local potentials.[10),11)] The introduction of such potentials enables us to reconstruct

*) The preliminary work has been reported in reference 1).

**) Now at Department of Physics, Nagoya University, Nagoya.

***) Now at Simulator Laboratory, Hokkaido University, Sapporo.

the α-particle model by treating systems dynamically,[7] and gives a reasonable way for the description of α-cluster structure on the basis of the two-nucleon forces.

Recent studies have brought about increasing recognitions for the importance of α-like four-body correlation or molecular structure in *sd*-shell nuclei. Arima, Horiuchi and Sebe have proposed a weak-coupling model[12] for the core excited states in light nuclei, in relating to the α-cluster model. Marumori and Suzuki have presented a microscopic theory[13] of α-like four-body modes, in order to describe the deformed excited states in light closed shell nuclei. A preliminary analysis[1] has also been made for the nuclei around ^{20}Ne in terms of an α-cluster plus ^{16}O-core model, by the present authors. Very recently, Eichler, Marumori and Takada have discussed[14] the basic assumption of the weak-coupling model in the framework of the theory of α-like four-body modes. Also, Horiuchi and Ikeda have suggested[15] a molecule-like structure (an α-particle plus a residual core nucleus) in light $4n$-nuclei, on the basis of the study of the $K^\pi=0^\pm$ rotational bands.

In order to clarify further the importance of α-like four-body correlations or molecular aspects in *sd*-shell nuclei, it is very desirable to investigate to what extent the picture of α-clustering is applicable to low-energy states of the nuclei. The main purpose of this paper is to examine a possibility of the α-cluster structure in ^{20}Ne and neighboring nuclei such as ^{19}F and ^{21}Ne, on the basis of the α-clustering picture which is capable of dynamical treatments of the systems.

A possible way of such approach is given by the α-particle model mentioned above. Then, the α-cluster plus ^{16}O-core model is proposed for the present purpose as follows. Let us put four nucleons (two neutrons and two protons) on a closed shell ^{16}O core. It is assumed that they localize to form a stable α-cluters which interacts with the ^{16}O core through an effective α-^{16}O potential. This interaction is supposed to be weak, so that an average nuclear field produced by the ^{16}O core may not be much disturbed by the existence of the α-cluster. Therefore, when particles or holes are added to this system and when particle-hole pairs are created from the ^{16}O core, they move in the average nuclear field, interacting with the α-cluster through an effective N-α potential.

The essential point of the present approach is to stand on the assumption of *weak coupling* between the α-cluster and the ^{16}O core. The effective α-^{16}O (N-α) potential is introduced so as to include effects of the Pauli principle operating between the α-cluster and the ^{16}O core (the nucleon and the α-cluster). It should be noted that the present model does not start from the picture of five closely packed α particles.

In § 2, the formulation of the model is given. The model Hamiltonian describes the motions of the coupled system of fermions and a *boson*. The model is, in many respects, analogous to the unified model,[16] developed by Bohr and Mottelson, which incorporates individual particle motion and collective motion,

The description of single-particle states is also given. In § 3, the effective N-α potential is chosen and its matrix elements are given in a suitable representation. In relation to the N-α partial waves of the single-particle wave function, effects of the Pauli principle operating between the nucleon and the α-cluster are discussed. This effects are suitably taken into account by the s-state N-α repulsion, in the adiabatic limit. In § 4, the motion of the α-cluster around the ^{16}O core is considered. The effective α-^{16}O potential is determined from the study of the $K^\pi=0^\pm$ rotational bands of ^{20}Ne $(\alpha+^{16}O)$. In §§ 5 and 6, the motions of a hole and a particle are investigated, respectively, in terms of the effective N-α potential. The low-lying anomalous-parity states of ^{19}F $(\alpha+^{16}O+h)$ and the ground rotational band of ^{21}Ne $(\alpha+^{16}O+p)$ are described with weak- and strong-coupling schemes, respectively, where the hole takes spherical p orbitals and the particle moves deformed sd ones. In § 7, the motion of a particle-hole pair is analyzed. The $K^\pi=2^-$ rotational band of ^{20}Ne $(\alpha+^{16}O+p+h)$ is studied with the strong-coupling scheme, where $(p_{1/2})^{-1}d_{5/2}$ configurations are treated with p-h interactions. Finally, in § 8, the summary and conclusion of this paper are given.

§ 2. Formulation of the model

2. 1) *Model Hamiltonian*

An α-cluster plus ^{16}O-core model is constructed on the basis of the following picture and is applied to the nuclei with mass numbers $A=19$, 20 and 21. Some low-energy states of these nuclei are considered to be described by the coupling of the relative motion between an α-cluster and a closed-shell ^{16}O core with the motions of particle and hole in an average nuclear field produced by the ^{16}O core. Therefore, this model deals with the coupled system of fermion and *boson* motions.

It is assumed that four nucleons on the outside of the ^{16}O core form a stable α-cluster. Then, we introduce effective α-^{16}O and nucleon (N)-α potentials, together with the average nuclear field and residual forces for the remaining nucleons.

The Hamiltonian H of the coupled system may be written as

$$H=H_N+H_\alpha+H_I+U+E_\alpha\,, \tag{2·1}$$

where H_N, H_α and H_I denote the fermion, *boson* and coupling terms, respectively, U is the internal energy of the ^{16}O core and E_α that of the α-cluster.

The fermion term H_N describes the $(A-4)$ nucleon system and is assumed to be represented by the shell model with residual forces. A single-particle state is denoted by a set of quantum numbers α. Let us introduce the Fermi operator c_α^+ (c_α) which creates (destroy) a nucleon in the state α. It is convenient to express H_N by means of the particle-hole representation. Choosing the ^{16}O core as a vacuum ϕ_0, we can write H_N as

$$H_N=\sum_{\alpha}\varepsilon_{\alpha}N(c_{\alpha}^{+}c_{\alpha})+(1/2)\sum_{\alpha,\beta,\alpha',\beta'}(\alpha\beta|v|\alpha'\beta')N(c_{\alpha}^{+}c_{\beta}^{+}c_{\beta'}c_{\alpha'}),\qquad(2\cdot2)$$

where ε_{α} and v denote the single-particle energy and the residual force, respectively. The notation N represents the normal products[17] of the particle and hole operators with respects to ϕ_0. The matrix element for v is taken as

$$(\alpha\beta|v|\alpha'\beta')=\int\varphi_{\alpha}^{*}(1)\varphi_{\beta}^{*}(2)v(1,2)\varphi_{\alpha'}(1)\varphi_{\beta'}(2)d\tau_1d\tau_2,\qquad(2\cdot3)$$

where φ_{α} denotes the single-particle wave function.

The *boson* term H_{α} describes the motion of the α-cluster around the ^{16}O core:

$$H_{\alpha}=T+V_{\alpha C},\qquad(2.4)$$

where T and $V_{\alpha C}$ are the relative kinetic energy operator and the effective α-^{16}O potential, respectively.

The coupling term H_I gives rise to an interplay between the motion of the α-cluster and those of particles and holes, and is expressed as

$$H_I=\sum_{\beta,\beta'}(\beta|V_{N\alpha}|\beta')N(c_{\beta}^{+}c_{\beta'}),\qquad(2\cdot5)$$

where $V_{N\alpha}$ is the effective N-α potential. The matrix element for $V_{N\alpha}$ is defined by

$$(\beta|V_{N\alpha}|\beta')=\int\varphi_{\beta}^{*}(1)V_{N\alpha}(1,\alpha)\varphi_{\beta'}(1)d\tau_1,\qquad(2\cdot6)$$

which is a function of the dynamical variables for the α-^{16}O relative motion.

As mentioned before, the model is, in many respects, analogous to the unified nuclear model.[16] The coupling term (2·5) is treated in similar ways: for instance, it is treated in weak-coupling approximation to the hole motion in the $A=19$ system, while it is treated in strong-coupling approximation to the particle motion in the $A=21$ system.

2. 2) *Representations of the single-particle motion*

We denote the nucleon coordinate referring to the center of the average nuclear field by $\boldsymbol{r}$. The axis of quantization is chosen along a z axis fixed in space (see Fig. 1). In the *jj*-coupling scheme the single-particle wave function φ_{α} is defined by

$$\varphi_{\alpha}\equiv|nls;jm\tau)=R_{nl}(r)[Y_l(\hat{\boldsymbol{r}})\times\chi_s(\sigma)]_{jm}\chi_{\tau},\qquad(2\cdot7)^{*)}$$

$$[Y_l(\hat{\boldsymbol{r}})\times\chi_s(\sigma)]_{jm}=\sum_{m_l,m_s}(lsm_lm_s|jm)Y_{lm_l}(\hat{\boldsymbol{r}})\chi_{sm_s}(\sigma),\qquad(2\cdot8)$$

where Y_{lm_l}, χ_{sm_s} (χ_{τ}) and R_{nl} are the spherical harmonics, the spin (isospin) and radial wave functions, respectively, $(ab\alpha\beta|c\gamma)$ is the Clebsch-Gordan coefficient.

*) Hereafter, the isospin function and its quantum numbers are omitted unless they are necessary.

The quantum numbers are shown with the usual notation: n is the number of the radial node including the one at infinity, l the orbital angular momentum, j and m denote the total angular momentum and its projection on the z axis and τ specifies the charge states. All the phase conventions in the angular momentum algebra follow those of Condon and Shortley.[18]

The Fermi operators (c_α^+, c_α) are transformed into the particle and hole ones, (a_α^+, a_α) and (b_α^+, b_α), as follows:

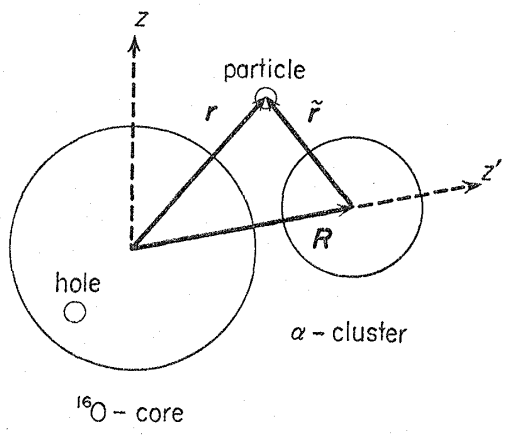

Fig. 1. The schematic representation of the coordinate systems in the α-cluster plus ^{16}O-core model.

$$c_\alpha^+ = (1-\theta_a)\, a_\alpha^+ + \theta_a (-)^p b_{-\alpha}\,, \tag{2·9a}$$

$$c_\alpha = (1-\theta_a)\, a_\alpha + \theta_a (-)^p b_{-\alpha}^+\,, \tag{2·9b}$$

where $\alpha = (nlj, m\tau) = (a, m\tau)$, $p = j-m+1/2-\tau$, θ_a is 1 or 0, according as the state j is occupied or not, and the choice of the phase factor follows Brown's.[19]

The single-particle states are so far described in the space-fixed frame. The α-cluster around the ^{16}O core defines the body-fixed frame in which a z' axis is taken as the α-^{16}O symmetry axis (see Fig. 1). We may also introduce the Fermi operators $(\gamma_\lambda^+, \gamma_\lambda)$ in the body-fixed frame and the corresponding particle and hole ones, $(\alpha_\lambda^+, \alpha_\lambda)$ and $(\beta_\lambda^+, \beta_\lambda)$, where $\lambda = (nlj, \Omega) = (a, \Omega)$ and Ω is now the projection of j on the z' axis. Then, these operators transform under rotations as

$$c_{am}^+ = \sum_\Omega D^j_{m\Omega}(\Theta_i)\, \gamma_{a\Omega}^+\,, \tag{2·10a}$$

$$c_{am} = \sum_\Omega D^{j}_{m\Omega}{}^*(\Theta_i)\, \gamma_{a\Omega}\,, \tag{2·10b}$$

where $D^j_{m\Omega}$ is the symmetric-top function[20] and Θ_j symbolizes the Eulerian angles specifying the orientation of the body axes in space.

As long as only a hole is considered (^{19}F or ^{19}Ne), its motion can suitably be described by means of the jj-coupling single-particle wave functions φ_α in the space-fixed frame (see § 5). In treating the motion of a particle (^{21}Ne or ^{21}Na), however, it becomes necessary to introduce another basic set ϕ_ρ defined in the body-fixed frame (see § 6). This is given in the $l\Lambda$-representation of Nilsson:[21]

$$\phi_\rho \equiv |nls, \Lambda\Sigma\Omega) = \phi_{nl\Lambda}(\boldsymbol{r}')\, \chi_{s\Sigma}(\sigma')\,, \tag{2·11}$$

$$\phi_{nl\Lambda}(\boldsymbol{r}') = R_{nl}(r)\, Y_{l\Lambda}(\hat{\boldsymbol{r}}')\,, \tag{2·12}$$

where $\Omega = \Lambda + \Sigma$, Λ and Σ are the components of the orbital and spin angular momenta along the z' axis, respectively, and the primed nucleon coordinates

referr to the body-fixed frame.

We will call the basic sets in the body-fixed frame the intrinsic states. In particular, the base ϕ_ρ plays important roles in the present model, since they enable us to take into account explicitly the effects of the coupling term H_I, as will be seen in the next section.

In the single-particle wave functions, (2·7) and (2·12), the radial functions R_{nl} are assumed to be approximately represented by the harmonic oscillator functions.[22] The size parameter of the oscillator, $b=(\hbar/M\omega)^{1/2}$ (M being the nucleon mass and $\hbar\omega$ the oscillator energy quantum), is determined from the high-energy electron scattering data.[23] The value is taken as $b=1.76$ fm for ^{16}O.

The single-particle energies ε_α are determined from the empirical values of energy spectra and binding energies around ^{16}O, under the assumption of the jj-coupling shell model.[19]

§ 3. The effective N-α potential and its matrix elements

3.1) *Choice of the effective N-α potential*

Interaction between a nucleon and an α-particle has state- and energy-dependent and non-local characters.[8] In the systems considered, the kinetic energy of the nucleons relative to the α-cluster is limited to low values, and only the states with low N-α relative angular momenta are available for the N-α interaction, as will be seen soon. Therefore, we introduce an effective N-α potential based on the phenomenological one[10] which is determined from the N-α elastic scattering process at low energies.

Phenomenological N-α potentials are known to have state-dependence and strong spin-orbit coupling.[10a] The interaction is strongly repulsive in the s state but attractive in the p state.[10b] It becomes less attractive as a whole in the d state.[8a] These characteristic features originate mainly from the Pauli principle.

Taking into account these features, we will choose the effective N-α potential $V_{N\alpha}$ in the coupling terms H_I of Eq. (2·5) as a sum of a zero-range delta spike, which acts on the s state only, and a p-state attractive Gaussian well with spin-orbit coupling:

$$V_{N\alpha}=A\delta(\tilde{\boldsymbol{r}})+V_0\exp(-a\tilde{r}^2)\{1+c\tilde{\boldsymbol{l}}\cdot\boldsymbol{s}\}, \tag{3·1}$$

where $\tilde{\boldsymbol{r}}$ denotes the N-α relative coordinate (see Fig. 1) and $\tilde{\boldsymbol{l}}$ the corresponding angular momentum operator. The strength A is determined so as to give a repulsive net contribution to the N-α relative s-state in the matrix elements (2·6) of $V_{N\alpha}$. The state-dependence of the attractive well is not yet taken into account in Eq. (3·1). This will be introduced for the matrix elements of $V_{N\alpha}$ between the intrinsic states in an approximate manner (see a next subsection and Eq. (3·6)).

It should be noted that the delta spike in Eq. (3·1) is introduced as an

effective force, in order to represent the effects of the *N-α short range correlations* due to the strong *s*-state repulsion. Correspondingly, in this paper the model space for the nucleon is truncated in the 1*s*, 1*p* and 2*s*-1*d* shells.

3. 2) *Roles of the N-α interaction*

Let us look at the *N-α* relative motions, where the nucleon is in the single-particle states of the ^{16}O core. This can be simply done in the body-fixed frame, if we take an extreme version of the adiabatic approximation, by expanding the intrinsic orbit (2·12) into the angular-momentum eigenstates referring to the *α*-cluster. Here, we assume that the motion of the nucleon in the average nuclear field is much more rapid than that of the *α*-cluster around the ^{16}O core, and also suppose that the latter two are well separated by an rms α-^{16}O distance d (this being expected from the shape of an effective α-^{16}O potential introduced in the next section). We then have

$$\phi_{\iota\Lambda}(\boldsymbol{r}') = \sum_{\tilde{l}} f_{\iota\tilde{l},\Lambda}(\tilde{r}, d)\, Y_{\tilde{l}\Lambda}(\hat{\tilde{\boldsymbol{r}}}'), \tag{3·2}$$

where the *N-α* partial waves $f_{\iota\tilde{l},\Lambda}$ are obtained by using the oscillator functions for R_{nl} in Eq. (2·12). As examples, $f_{1d\tilde{l},\Lambda}$ ($\Lambda=0, 1, 2$) are plotted against $\tilde{r}$ for various $\tilde{l}$ in Fig. 2 with $b=1.76$ fm and $d=4$ fm (b being the size parameter of R_{nl} and d being determined from the rms radius of ^{20}Ne in the next section).

The expansion (3·2) and Fig. 2 indicate the following facts. (1) The intrinsic orbits $\phi_{\iota\Lambda}$ (defined in the body-fixed frame) do not contain the *N-α*

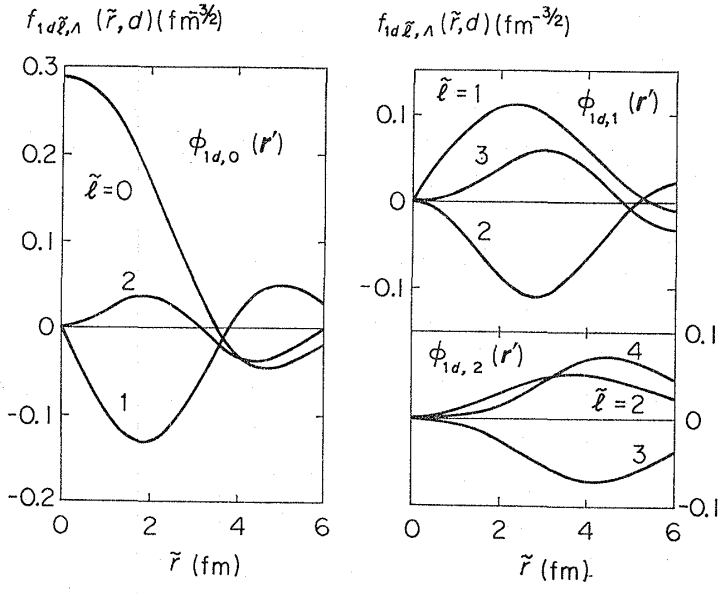

Fig. 2. The *N-α* partial waves $f_{1d\tilde{l},\Lambda}(\tilde{r}, d)$ of the intrinsic orbit $\phi_{1d,\Lambda}(\boldsymbol{r}')$, plotted against the *N-α* relative distance $\tilde{r}$ for various $\tilde{l}$. The size parameter b of the oscillator functions and the α-^{16}O rms distance d are taken as $b=1.76$ fm and $d=4.0$ fm.

relative angular-momentum state with $\tilde{l}$ smaller than $|\Lambda|$, since $f_{l\tilde{l},\Lambda}$ vanish identically for $\tilde{l}<|\Lambda|$. (2) For the adopted values of the parameters b and d, it is only for the low values of $\tilde{l}$ that $f_{l\tilde{l},\Lambda}$ have appreciable amplitudes within the range of the N-α interaction ($\tilde{r}\lesssim 4$ fm). (3) In the $\Lambda=0$ cases, $f_{l0,0}$ (the s waves) have a large amplitude in the region of small $\tilde{r}$. (4) In the $\Lambda\neq 0$ cases, $f_{l\tilde{l},\Lambda}$ have comparable magnitudes in the same region, especially in the case $\Lambda=l$ (e.g. $f_{1p\tilde{l},1}$ with $\tilde{l}=1$ and 2 or $f_{1d\tilde{l},2}$ with $\tilde{l}=2$ and 3).

These facts enable us to understand the roles of the N-α interaction *in the adiabatic limit*. From the facts (1) and (2) we can see that, in the intrinsic orbits $\phi_{l\Lambda}$ considered, what parts of the N-α partial waves are important to the N-α interaction.

The fact (3) suggests a relation between the N-α s-state repulsion and the Pauli principle. The behaviors of $f_{l0,0}$ at small $\tilde{r}$ are not compatible with the existence of the s-state nucleons in the α-cluster. In the present approach, however, this difficulty is solved by introducing the strong s-state N-α repulsive force. Then, it mixes the s-waves $f_{l0,0}$ of the various ϕ_{l0} and brings about the damping of the N-α relative s-state part at small $\tilde{r}$ in the total wave function.*) This gives rise to also the *polarization* of the ^{16}O-core state, as well as the N-α *short range correlations* in the states of the nucleon. Actually, as mentioned before, these effects are represented with the effective forces acting on the *unpolarized* ^{16}O-core and on the *uncorrelated* particle and hole in the truncated space (i.e. the effective α-^{16}O potential $V_{\alpha O}$ in Eq. (2·4) and the delta spike of $V_{N\alpha}$ in Eq. (3·1), respectively).

The fact (4) tells us an approximate way of taking into account the state-dependence of the N-α attraction. Denoting the N-α p-state attractive well by V_p, we consider the matrix element $(\phi_{1d,1}, V_p\phi_{1d,2})$, as an example. This element does not contain the contributions from the N-α relative s and p states. Therefore, we must multiply it by a reduction factor (the N-α d-state interation being less attractive than the p-state one).

3. 3) *Matrix elements for the effective N-α potential*

In order to represent explicitly the effects of the N-α s-state repulsion and to take into account properly the state-dependence of the N-α attractive well, we express the coupling term H_I of Eq. (2·5) in terms of the intrinsic states. To do so, it is convenient to express $V_{N\alpha}$ of Eq. (3·1) in terms of the nucleon coordinate $\boldsymbol{r}$ and the α-^{16}O relative coordinate $\boldsymbol{R}$ (see Fig. 1). Then, we obtain

---

*) This is also suggested from the same arguments as those in the N-α and α-α systems.[8),9)] When the antisymmetrization is completely performed in the total system including the four nucleons in the α-cluster, it may be expected that the spurious part of the s-waves $f_{l\,0,\,0}$, which violates the Pauli principle, is excluded and that the remaining physical part behaves as if there were a repulsive force.

$$V_{N\alpha}=A\delta(\boldsymbol{r}-\boldsymbol{R})+\exp\{-a(\boldsymbol{r}-\boldsymbol{R})^2\}\cdot[1+(4c/5)\{(\boldsymbol{l}\cdot\boldsymbol{s})+([\boldsymbol{p}\times\boldsymbol{R}]\cdot\boldsymbol{s})\}+(c/4)\{(\boldsymbol{L}\cdot\boldsymbol{s})-([\boldsymbol{r}\times\boldsymbol{P}]\cdot\boldsymbol{s})\}], \quad (3\cdot3a)^{*)}$$

$$\equiv V^{(s)}+\sum_{k=0}^{4}V^{(k)}, \quad (3\cdot3b)$$

where $\boldsymbol{p}$ and $\boldsymbol{P}$ are the canonical momenta for $\boldsymbol{r}$ and $\boldsymbol{R}$, respectively, $\boldsymbol{l}$ and $\boldsymbol{L}$ being the corresponding orbital angular momenta.

Under the adiabatic approximation we can put $\boldsymbol{P}$ or $\boldsymbol{L}$ equal to zero in the non-central parts $V^{(k)}$ of Eq. (3·3a). Then, by making use of the transformations (2·10), we can rewrite the coupling term (2·5) in the form

$$H_I=\sum_{\lambda\lambda'}(\lambda|\overline{V}_{N\alpha}|\lambda')_b N(\gamma_\lambda{}^+\gamma_{\lambda'}) \quad (3\cdot4)$$

with

$$(\lambda|\overline{V}_{N\alpha}|\lambda')=\sum_{\Lambda\Sigma,\Lambda'\Sigma'}(ls\Lambda\Sigma|j\Omega)\times(l's\Lambda'\Sigma'|j'\Omega')(\rho|\overline{V}_{N\alpha}|\rho')_b, \quad (3\cdot5)$$

$$(\rho|\overline{V}_{N\alpha}|\rho')_b=(1/2)\xi(\Lambda)\times[(\rho|V_{N\alpha}|\rho')_b+(\rho'|V_{N\alpha}|\rho)_b], \quad (3\cdot6)$$

where $\lambda=(nlj,\Omega)$, $\rho=(nl,\Lambda\Sigma)$ and the suffix b means that the matrix elements are defined in the body-fixed frame under the adiabatic limit, the symmetrization being required to preserve the Hermiticity of H_I.

Following the argument in the previous subsection, the state-dependent factor $\xi(\Lambda)$ is introduced in Eq. (3·6). For the matrix elements involving the N-α s-state contributions we take $\xi(\Lambda=0)=1$. For the other elements we treat $\xi(\Lambda\neq0)$ as free parameters not larger than unity.

The expressions of $(\rho|V_{N\alpha}|\rho')_b$ are obtained with the aid of the tensor algebra.[24] It should be noted that

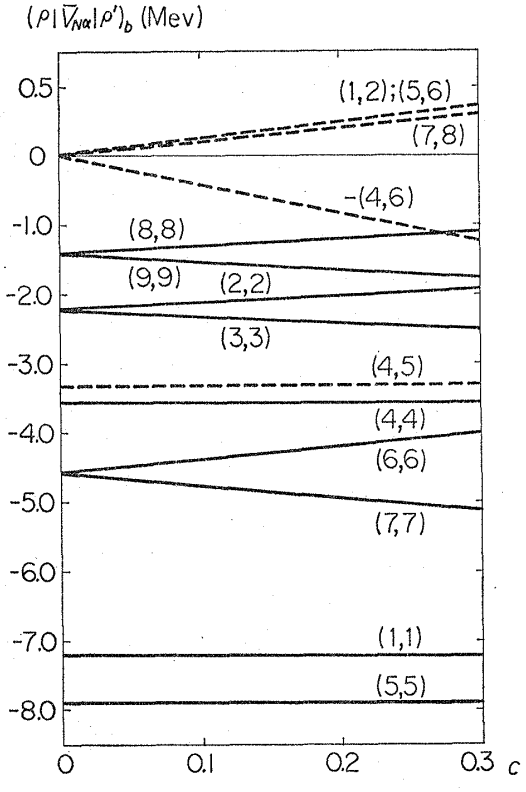

Fig. 3. The N-α matrix elements $(\rho|\overline{V}_{N\alpha}|\rho')_b\equiv(\rho,\rho')$ plotted against the spin-orbit coupling strength c for the $1p$ and $2s$-$1d$ shells, where $\rho=1$, 2, ..., and 9 mean $(l\Lambda\Sigma)=(p0+)$, $(p1-)$, $(p1+)$, $(s0+)$, $(d0+)$, $(d1-)$, $(d1+)$, $(d2-)$ and $(d2+)$, respectively. The values of the potential parameters involved are taken as $V_0=-47.32$Mev, $a=0.189$ fm^{-2}, $A=0$ and $\xi(\Lambda)=1$. The values of b and $R=d$ are the same as those in Fig. 2.

*) The non-central parts $V^{(k)}$ ($k=1\sim4$) are derived for the case of the $A=20$ ($\alpha+^{16}O$) system by regarding the relevant momentum operators as classical quantities, and they are also applied to the $A=19$ or 21 ($\alpha+^{16}O+h$ or p) system.

$(\rho|V_{N\alpha}|\rho')_b$ do not have non-diagonal elements with respect to Ω $(=\Lambda+\Sigma)$, the projection of j on the z' axis. The delta spike in $V_{N\alpha}$ has non-vanishing elements only for the intrinsic states with $\Lambda=0$. Furthermore, $(\rho|V_{N\alpha}|\rho')_b$ are obtained as a function of R, the α-^{16}O distance.

For the $1p$ and $2s$-$1d$ shells $(\rho|\overline{V}_{N\alpha}|\rho')_b$ are plotted against c, the spin-orbit strength of $V_{N\alpha}$, in Fig. 3, where $b=1.76$ fm, $R=d=4$ fm and the values of the potential parameters are taken as those of the p-state N-α potential:[10a] $A=0$, $\xi=1$, $V_0=-47.32$ Mev, $a=0.189$ fm^{-2} (and $c=0.248$) in Eq. (3·1).

§ 4. The $K=0$ rotational bands in ^{20}Ne

Motion of the α-cluster and the effective α-^{16}O potential

Many overlapping rotational bands have been confirmed experimentally in ^{20}Ne.[25] In this section we are interested in the ground $K^\pi=0^+$ and the excited $K^\pi=0^-$ bands. The former band which has the sequence of the spin and parity $L^\pi=0^+$, 2^+, $\cdots$ has been investigated in many theoretical studies[4),26)] based on the $(sd)^4$ configuration. The latter band which has the sequence $L^\pi=1^-$, 3^-, $\cdots$ and starts from the 5.80 Mev excitation has been interpreted as the $K^\pi=0^-$ octupole b-vibrational band[25] or the band on the $(sd)^3(pf)^1$ configuration.[27]

In the present model the two bands are interpreted as the states due to the orbital motions of the α-cluster. It may be assumed that the motions are determined through an effective α-^{16}O potential, phenomenologically.

4. 1) *Choice of the effective α-^{16}O potential*

Interaction between α particles provides one of the typical examples for such potentials. It has been established that energy-independent but state-dependent local potentials with repulsive cores can well describe the α-α scattering at low energies.[11] Investigations[9] based on the two-nucleon forces have clarified that the features of the effective α-α potentials are attributed to the many-body structure of the whole system in the full overlap region of the α particles and to the non-local character of the interaction due to the antisymmetrization among the nucleons involved.

Therefore, it may be expected that relative motions between an α-particle and other stable clusters can be also approximately described with effective local potentials having a repulsive core and a state-dependent outer attractive well.

We denote the effective α-^{16}O potential $V_{\alpha O}$ for the state with the relative angular momentum L by $V_L(R)$, where $\boldsymbol{R}$ is the α-^{16}O relative coordinate. A square well potential with a hard core is adopted for $V_L(R)$, as the simplest one with the required features. The range R_0 of the well is estimated from the one-pion-exchange range and rms radii[23] of ^{4}He and ^{16}O: $R_0=1.4$ fm $+\langle r^2\rangle_\alpha^{1/2}+\langle r^2\rangle_{^{16}O}^{1/2}=5.7$ fm. The state-dependent well depth V_L and the hard core radius R_C are determined so as to reproduce consistently the experimental values of the

binding energies, rms radius and electric quadrupole ($E2$) transitions within the bands.

4. 2) *Description of the rotational bands*

Each state of the $K=0$ bands is described by means of the *boson* term H_α of Eq. (2·4):

$$\{T+V_L(R)-E_L\}\chi_L(R)\,Y_{LM_L}(\hat{\boldsymbol{R}})=0\,, \tag{4·1}$$

where χ_L is the α-^{16}O radial function and the eigenvalue E_L is written as $E_L=E(L)+\text{B.E.}(^4\text{He})+\text{B.E.}(^{16}\text{O})-\text{B.E.}(^{20}\text{Ne})$, $E(L)$ being the excitation energy in ^{20}Ne.

In solving Eq. (4·1) we treat effects of the α-^{16}O Coulomb force as a perturbation energy $E_C(\alpha\text{-}^{16}\text{O})$. This is estimated as $E_C(\alpha\text{-}^{16}\text{O})=4.5$ Mev, by assuming the uniform charge densities for ^{4}He, ^{16}O and ^{20}Ne.

The rms radius of ^{20}Ne can be written as

$$\langle r^2\rangle_{^{20}\text{Ne}}=(4/25)\,d^2+(1/5)\langle r^2\rangle_\alpha+(4/5)\langle r^2\rangle_{^{16}\text{O}}\,, \tag{4·2}$$

where $d^2=\langle R^2\rangle$ is the rms α-^{16}O distance and $d_{\text{exp}}=4.0$ fm if $\langle r^2\rangle_{^{20}\text{Ne}}=(2\cdot9\text{ fm})^2$ is used which is calculated with the value 3.8 fm for the radius of the uniform charge distribution of ^{20}Ne through the empirical formula[23] for nuclear sizes.

The $E2$ operator for the α-^{16}O relative motion is given by

$$E(2,q)=(8/5)\,eR^2Y_{2q}(\hat{\boldsymbol{R}})\,. \tag{4·3}$$

The reduced $E2$ transition probabilities within the same band are given by the well-known formula[22]

$$B(E2;L\to L')=(5/16\pi)\,Q^2(L',L)\,(L200|L'0)^2, \tag{4·4}$$

where

$$Q(L',L)=(16/5)\,e\,(\chi_{L'}|R^2|\chi_L)\,. \tag{4·5}$$

The typical examples of the effective α-^{16}O potentials $V_L(R)$ determined for the $L=S$, D, G states are plotted against R in Fig. 4. The corresponding values of $B(E2)$ are listed in Table I and compared with the experimental data.[23]

As is well known, in ^{20}Ne the rotational spectrum and the $E2$ transition rates deviate considerably from the predictions of the rotational model.[20] In the ground band we have $R_E=0.79$ and $R_B=0.60$, where R_E and R_B are the ratios of the experiments to the rotational model for $E(G)/E(D)$ and $B(E2;G\to D)/B(E2;D\to S)$, respectively.

We can see that the repulsive core and state-dependence of $V_{\alpha C}$ give a

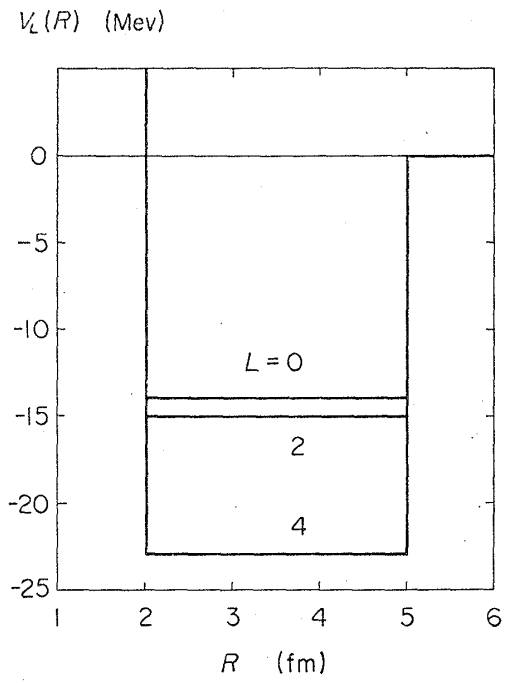

Fig. 4. The nuclear parts of the effective α-^{16}O potentials, $V_L(R)$, plotted against the α-^{16}O relative distance R for the $L^\pi=0^+$, 2^+ and 4^+ states. They are determined from the binding energies, rms radius and $E2$ transition rates of the corresponding states within the ground rotational band in ^{20}Ne.

Table I. The reduced $E2$ transition probabilities within the ground rotational band in ^{20}Ne. The calculated values are obtained in terms of the radial functions $\chi_L(R)$ determined from the potentials $V_L(R)$ which are shown in Fig. 4.

L	L'	$(L'\|R^2\|L)^{1/2}$ (fm)	$B(E2;\ L\to L')$ $(e^2\mathrm{fm}^4)$	
			Cal	Exp[23]
2^+	0^+	4.07	55.6	57.3
4^+	2^+	3.61	49.6	49.7

consistent understanding for the deviations of R_E and R_B from unity.*) As shown in Fig. 4, the well depths V_S and V_D are determined to be nearly equal. The radial functions χ_S and χ_D have little difference, because of the large hard core radius $R_C(\gtrsim 2\,\mathrm{fm})$. On the other hand, V_G is determined as $|V_G|>|V_S|$ and $|V_D|$, in order to make $R_E<1$. As a consequence, χ_G is pushed into more inner region. This makes also $R_B<1$, as shown in Table I.

From the observed energy gap between the $K^\pi=0^+$ and 0^- bands, it is apparent that the attractive parts of $V_{\alpha G}$ for the $L=$odd states should be systematically weakened as compared with those for the $L=$even states. A possible explanation may be given by the differences of the many-body structures and non-local interactions in the $L=$even and odd states. However, this problem has not yet been investigated, although the N-α interaction provides a typical example.

In this connection, for the $K^\pi=0^\pm$ rotational bands in ^{16}O* and ^{20}Ne an excellent interpretation has recently been proposed,[15] in which the two bands are unified as a twin with the same molecule-like structure (an α-particle plus a residual core nucleus) and the energy gap of the two bands is explained as the splitting energy of a reflection doublet.

*) In this respect, the following should be noted. As long as we stand on the picture of the structureless α-particle, the state-dependence of $V_{\alpha G}$ is never obtained. That is, the vacuum expectation value for a simple sum of the effective N-α potential $V_{N\alpha}$,

$$V_{\alpha G}^{(0)}(R)=\langle\phi_0|\Sigma_{\beta\beta'}(\beta|V_{N\alpha}|\beta')c_\beta{}^+c_{\beta'}|\phi_0\rangle, \qquad (4\cdot6)$$

becomes essentially state-independent, although it has a repulsive core only due to the s-state repulsion of $V_{N\alpha}$.

§ 5. The low-lying anomalous-parity states in ^{19}F

Motion of a hole

5.1) *Weakening of the hole-α interaction*

Several studies[29] have been made to explain the low-lying anomalous-parity levels in ^{19}F. There is the famous $1/2^-$ state at the 0.11 Mev excitation. Recently, a consideration for the binding energy of this level has led to the weak-coupling model,[12] which is based on the assumption that the interaction between a $p_{1/2}$ hole and four particles in the *sd* shell is rather weak. Physical reason for the weakening of the effective $1h$-$4p$ interaction has been clarified[14] in the framework of the microscopic theory,[13] where the weakening effects are essentially caused by the complex ground state correlations due to the α-like four-body modes.

In the present model this weak-coupling phenomenon can be understood as a result of the characteristic features of the N-α interaction. In fact, in the $j\Omega$ representation the matrix elements (3·5) of the effective N-α potential $V_{N\alpha}$ become small, if we choose the strength A and the state-dependent factor $\hat{\xi}$ suitably in Eq. (3·6). To show this, for the p-shell proton the elements $(\lambda|\overline{V}_{N\alpha}|\lambda')_b$ are plotted against the spin-orbit strength c in Fig. 5. Here, the solid lines are obtained in terms of $A/(\sqrt{\pi}b)^3=100$ Mev and $\hat{\xi}(\Lambda=1)=0.7$, and the dotted lines correspond to the cases $A=0$ and $\hat{\xi}=1$. The values of other parameters involved are the same as those in Fig. 3, the contributions from the proton-α Coulomb force V_C being calculated as $(1p0|V_C|1p0)_b=0.75$ Mev and $(1p1|V_C|1p1)_b=0.60$ Mev.

As seen from the A-dependence in Fig. 5, the weakening of the h-α interaction originates from the characteristic of the N-α interaction, that is the s-state repulsion, and also from the behavior of the N-α partial waves of the intrinsic orbits, which is discussed in § 3. A hole in the jj-coupling single-particle states can interact with the α-cluster through the relative s and other states simultaneously. Hence, the contributions from the s-state repulsion and the attractions in the other states cancel each other.

The present model apparently suggests an alternative understanding of the mechanism for the weakening of the effective $1h$-$4p$ interaction.

5.2) *Basic vectors and energy matrices*

Since the coupling term H_I given by Eq. (3·4) becomes weak, the motions of the hole and the α-cluster are approximately independent and the hole moves on the spherical orbitals of the jj-coupling shell model. Then, the states of the $\alpha+^{16}O+h$ system are described with the basic vectors of the weak-coupling scheme:

$$|S;JM\rangle\equiv|L,a^{-1};JM\rangle=\chi_L(R)\,[Y_L(\hat{\boldsymbol{R}})\times b_\alpha{}^+]_{JM}|\phi_0\rangle\,, \qquad (5\cdot1)$$

where J denotes the total spin of the system, $\alpha=(nlj,m)=(a,m)$, the hole operators $(b_\alpha{}^+, b_\alpha)$ are defined in Eqs. (2·9) and the radial function χ_L is the solution of Eq. (4·1).

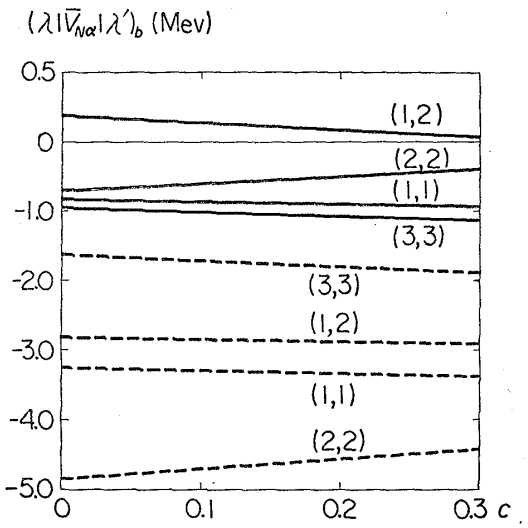

Fig. 5. The N-α matrix elements $(\lambda|\bar{V}_{N\alpha}|\lambda')_b \equiv(\lambda, \lambda')$, plotted against the spin-orbit coupling strength c for the $1p$-shell proton, where $\lambda=1$, 2 and 3 mean $(lj\Omega)=(p_{1/2}, 1/2)$, $(p_{3/2}, 1/2)$ and $(p_{3/2}, 3/2)$, respectively. The solid lines are calculated with $A/(\sqrt{\pi}b)^3=100$ Mev and $\xi(A=1)=0.7$. The dotted lines are obtained with $A=0$ and $\xi=1$. The contributions from the proton-α Coulomb force V_C are included as $(1p0|V_C|1p0)=0.75$ Mev and $(1p1|V_C|1p1)=0.60$ Mev. The values of the other parameters involved are the same as those in Fig. 3.

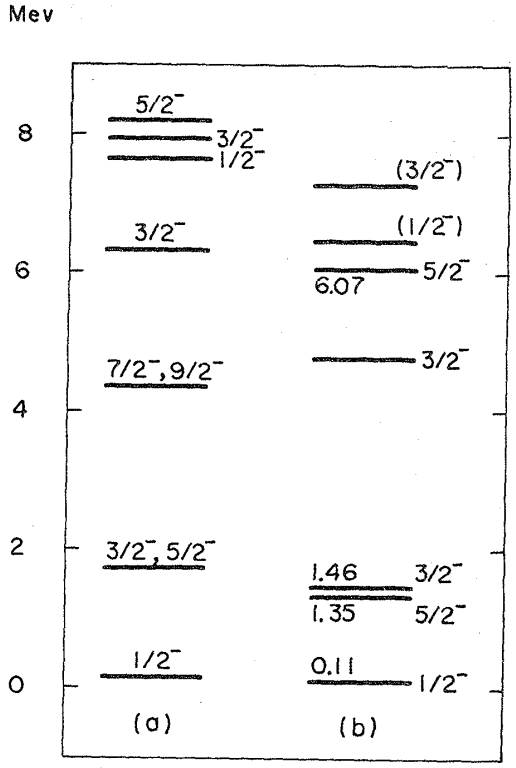

Fig. 6. Negative parity levels of ^{19}F, given relative to the observed binding energy of the $1/2^+$ ground state. (*a*) Calculated spectrum, based on the $p_{1/2}$ and $p_{3/2}$ hole configurations. The N-α matrix elements shown in Fig. 5 are used with $c=0.25$. (*b*) Experimental spectrum.[31]

The matrix elements of the total Hamiltonian (2·1) between the weak-coupling bases (5·1) are given by

$$\langle S; JM|H|S'; JM\rangle = \{-\text{B.E.}(^{20}\text{Ne}) - \varepsilon_j + E(L)\}\delta(Lj, L'j') - \langle S; J|V_{h\alpha}|S'; J\rangle, \tag{5·2}$$

with $\delta(ab\cdots, a'b'\cdots)=\delta_{aa'}\delta_{bb'}\cdots$. Here, the last term denotes the h-α matrix element which is related to the p-α one in the usual way:[30]

$$\langle S; J|V_{h\alpha}|S'; J\rangle = \sum_{J'}(2J'+1)\,W(Lj'jL'; J'J)\,(j'L; J'|V_{N\alpha}|jL'; J'), \tag{5·3}$$

where $W(abcd; ef)$ is the Racah coefficient. The p-α matrix elements of Eq. (5·3) can be expressed in terms of the matrix elements (3·5) under the adiabatic approximation. We then have

$$\langle S; J|V_{h\alpha}|S'; J\rangle = -\sum_{\Omega,\Omega'}(jJ-\Omega\Omega|L0)\,(j'J-\Omega'\Omega'|L'0)\,(\lambda|\bar{V}_{N\alpha}|\lambda')_{b,R=d}, \tag{5·4}$$

where the overlap integral with respect to χ_L and $\chi_{L'}$ is approximated by the values of $(\lambda|\bar{V}_{N\alpha}|\lambda')_b$ (a function of R) at the rms α-^{16}O distance d.

5. 3) *Energy spectra*

The energies of the negative parity states in ^{19}F are calculated in terms of the N-α matrix elements shown in Fig. 5, the values being taken at $c=0.25$ (which is equal to that of the free N-α potential[10a]). We use the experimental values for the single-particle and rotational excitation energies, ε_j and $E(L)$. Effects due to the non-diagonal elements of H_I are small and so the mixing of the basic configurations (5·1) is ignored.

The energy spectra originating from $p_{1/2}$ and $p_{3/2}$ hole configurations are shown in Fig. 6 and is compared with the experimental data.[31] The energies are given relative to the observed binding energy of the $1/2^+$ ground state.

Under the adiabatic approximation, the perturbation energies for the $p_{1/2}$ hole configuration become independent of J and are commonly given by $(p_{1/2}1/2|\overline{V}_{N\alpha}|p_{1/2}1/2)_b$. The resulting levels are essentially the same as those of the weak-coupling model.[12]

The experimental information from the $^{20}Ne(t, {}^4He)^{19}F$ reaction has indicated evidences[32] of the p-shell proton hole state in the region of about 5~7 Mev excitations. These levels may be considered to be formed by the coupling of the $p_{3/2}$-hole with the ^{20}Ne $(\alpha+{}^{16}O)$ core. As seen from Fig. 6, agreements are not very good. Further analyses free from the adiabatic approximation should be performed.

§ 6. The ground rotational band in ^{21}Ne

Motion of a particle

6. 1) *Basic vectors and energy matrices*

The low-lying positive parity states in ^{21}Ne have been known to exhibit the rotational character, and have been investigated in terms of the collective models[33] and the method of deformed orbitals.[4]

In the present model, also, a particle is considered to move on deformed intrinsic orbitals compatible with the Pauli principle operating between the particle and the α-cluster, and is described with the strong-coupling scheme in the body-fixed frame. Then, the states of the $\alpha+{}^{16}O+p$ system are represented by the following molecular-type wave functions as the basic vectors:

$$|B; JM\rangle \equiv |\rho, JMK=\Omega, \Pi=\pm\rangle = \sqrt{(2J+1)/16\pi^2}\,\chi(R) \times \{D^J_{MK}(\Theta_i)\alpha_\rho{}^+ \pm (-)^{J+s}D^J_{M-K}(\Theta_i)\alpha_{-\rho}{}^+\}|\phi_0\rangle \qquad (6\cdot1)$$

with $\rho=(nl, \Lambda\Sigma)$ and $\Omega=\Lambda+\Sigma$, where J denotes the total spin of the system, M and K are its projections on the space z axis and the body z' one (the symmetry axis of the ^{20}Ne $(\alpha+{}^{16}O)$ core), respectively, and Π the parity. The basic function (6·1) is separated into three parts: the rotational part, indicated by the D function (Θ_i being the Eulerian angles of the body axes); the vibrational part, denoted by χ, which represents the radial dependence of the α-^{16}O

relative motion; the nucleonic part, specified by $\alpha_\rho{}^+|\phi_0\rangle$, which describes the particle motion in the intrinsic state (2·11) ($(\alpha_\rho{}^+, \alpha_\rho)$ being the corresponding particle operators). Furthermore, in Eq. (6·1), $K=\Omega$ implies the axial symmetry of the system and the second term arises from the parity projection.

The basic vector (6·1) can be expressed in the space-fixed frame in terms of the following transformation:

$$|B; JM\rangle = \sum_{Lj} C_{SB}|S; JM\rangle\,, \tag{6·2}$$

where

$$C_{SB}\equiv C^J_{Lj}(\rho, \Pi=\pm) = [1\pm(-)^{L+l}]/\sqrt{2}\cdot(-)^{j+\Omega}(ls\Lambda\Sigma|j\Omega)\,(Jj-\Omega\Omega|L0)\,, \tag{6·3}$$

and the vector $|S; JM\rangle = |L, a; JM\rangle$ is defined by an expression similar to Eq. (5·1) with $a_\alpha{}^+$ instead of $b_\alpha{}^+$.

The matrix elements of the total Hamiltonian (2·1) between the strong coupling bases (6·1) are calculated with the aid of the transformation (6·2). Then, we wet

$$\begin{aligned}\langle B;JM|H|B';JM\rangle &= -\text{B.E.}(^{20}\text{Ne})\,\delta(\rho,\rho')\\ &+\sum_j (ls\Lambda\Sigma|j\Omega)\,(ls\Lambda'\Sigma'|j\Omega)\,\varepsilon_j\,\delta(nl\Omega, n'l'\Omega')\\ &+(\rho|\overline{V}_{N\alpha}|\rho')_{b,R=a}+\sum_{Lj} C_{SB}C_{SB'}E(L)\,\delta(nl, n'l')\,,\end{aligned} \tag{6·4}$$

where the N-α matrix elements are taken in the same way as that treated in Eq. (5·5). In deriving the last term which involves the rotational excitation energy $E(L)$ of the ^{20}Ne core, we have assumed that the vibrational function χ in Eq. (6·1) satisfies Eq. (4·1) for the *boson* term H_α. This is approximately valid, when the α-^{16}O relative motion is described by the effective α-^{16}O potential $V_{\alpha O}$ with the repulsive core, as seen in § 4.

In the matrix elements (6·4), the terms involving the N-α matrix elements and the single-particle energy ε_j determine a deformed intrinsic orbital $\psi(\Omega)$ of the particle with the spin projection Ω on the z' axis, while the terms involving the rotational energy $E(L)$ give, for $\Omega=\Omega'$, the rotational band belonging to $\psi(\Omega)$ and, for $\Omega\neq\Omega'$, the rotation-particle coupling which mixes different bands.

6. 2) *Wave functions and energy spectrum*

In the *sd* shell space we have six intrinsic states (2·11) specified by $(nl, \Lambda\Sigma)$. The states with $\Lambda=0$ are expected to appear with relatively higher energies than the other, because of the s-state N-α repulsion. When we take the strength A as $A/(\sqrt{\pi}b)^3=100$ Mev*) in $V_{N\alpha}$ of Eq. (3·1a), the N-α repulsive

*) This value gives a qualitatively consistent explanation for the binding energy of the d-shell hole state (the $3/2^+$ level at 0.15 Mev) in ^{43}Sc, as well as that of the p-shell hole state (the $1/2^-$ level at 0.11 Mev) in ^{19}F.

contributions are estimated as about 5 and 20 Mev for the states with $(nl, \Lambda) = (2s, 0)$ and $(1d, 0)$, respectively, $R=d=4$ fm being used. These contributions must be added to the corresponding elements shown in Fig. 3. The $(2s, 0)$ state does not have a sufficiently high energy, as compared with the $(1d, 0)$ one, and so the former state may play important roles in the excited band with $\Omega=1/2$. However, we are mainly interested in the ground band with $\Omega=3/2$. In this case the $(2s, 0)$ state have only minor effects, since it cannot couple with the ground band by the rotation-particle coupling (see Eq. (6·4)). Hence, the basic vectors (6·1) with $\Lambda=0$ can be excluded in a first approximation. Then, the state vectors are given by

$$|JM\rangle = \sum_{\Lambda=1,2,\Sigma=\pm} a_J(1d\Lambda\Sigma\Omega)\,|1d\Lambda\Sigma, JM\Omega\rangle\,. \qquad (6\cdot5)$$

In diagonalizing the energy matrix (6·4) with respect to the state vector (6·5), we use the experimental velues for ε_j and $E(L)$. The N-α matrix elements are calculated with $b=1.76$ fm and $d=4$ fm. The values of the parameters in $V_{N\alpha}$ are taken as $V_0=-50$ Mev, $a=0.195$ fm^{-2} and $c=0.2$, which are very close to those of the phenomenological p-state N-α potential.[10a] The state-dependent factor ξ in Eq. (3·6) is chosen as $\xi(\Lambda=1)=1$ and $\xi(\Lambda=2)=0$.

The resulting eigenvalues and eigenvectors are listed in Table II for the positive parity states with the various total spin J. The corresponding energy spectrum is shown in Fig. 7 and is compared with the experimental data[34] for ^{21}Ne. The energies are given relative to the observed energy of the $3/2^+$ ground state. To show the effects of the band mixing we present also the rotational spectra for the lowest bands with $\Omega=1/2$, $3/2$ and $5/2$ in Fig. 7. The lowest band with $\Omega=3/2$ is described by the deformed intrinsic orbital

$$\begin{aligned}\psi(\Omega=3/2) &= 0.973\phi(1d, 1+) + 0.233\phi(1d, 2-) \\ &= 0.974\varphi(1d_{5/2}, 3/2) + 0.227\varphi(1d_{3/2}, 3/2) \qquad (6\cdot6)\end{aligned}$$

for the adopted values of the parameters. The present model explains quite satisfactorily the observed energy spectrum of the ground band which consists of the states with $J^\pi=3/2^+$, $5/2^+$, $7/2^+$ and $9/2^+$ below 3 Mev excitations. For these states the mixing ratios of $\psi(\Omega=3/2)$ are estimated as about 83%.

Table II. The eigenvalues and eigenvectors for the ground band of ^{21}Ne. The energies are given relative to the observed binding energy of the $3/2^+$ ground state. The values of the various parameters, used in the calculations, are the same as those in Fig. 7.

J	$E(J)$ (Mev)	$a_J(1d1-)$	$a_J(1d1+)$	$a_J(1d2-)$	$a_J(1d2+)$
$3/2^+$	0.04	0.120	0.968	0.219	0
$5/2^+$	0.38	0.212	0.903	0.229	0.294
$7/2^+$	1.63	0.244	0.874	0.235	0.348
$9/2^+$	2.96	0.261	0.833	0.247	0.420
$11/2^+$	4.40	0.225	0.833	0.262	0.432

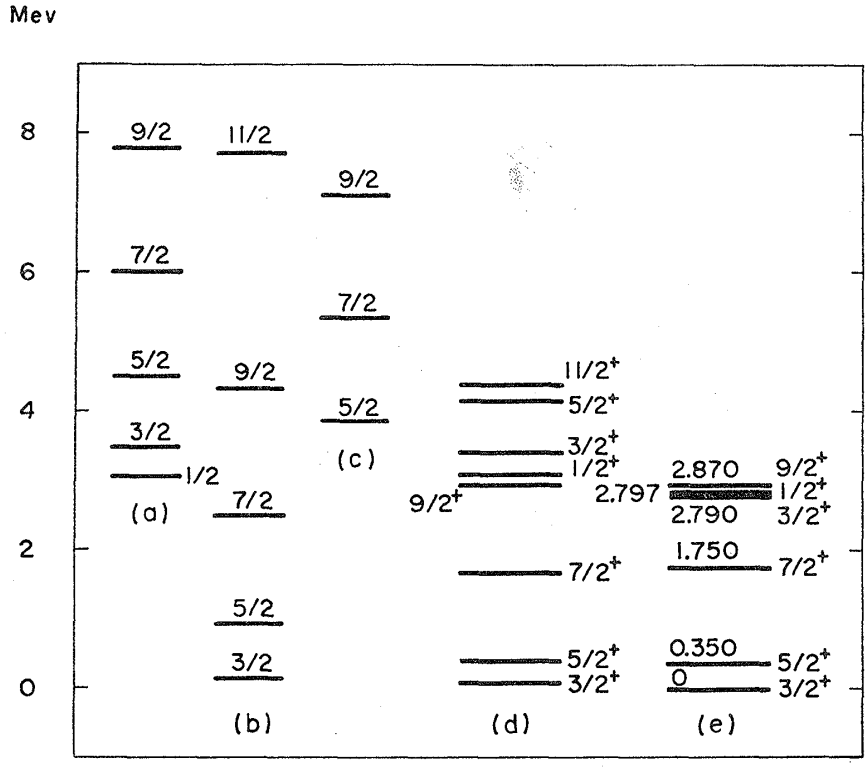

Fig. 7. Positive parity levels of ^{21}Ne, given relative to the observed binding energy of the $3/2^+$ ground state. (*a*), (*b*) and (*c*) indicate the rotational bands with $\Omega=1/2$, 3/2 and 5/2, respectively, based on the ($1d$, $\Lambda\neq 0$) particle configurations. (*d*) Calculated spectrum mixed by the rotation-particle coupling. (*e*) Experimental spectrum. In all calculations, $V_0=-50$ Mev, $a=0.195$ fm^{-2}, $c=0.2$, $\xi(\Lambda=1)=1$, $\xi(\Lambda=2)=0$, $b=1.76$ fm and $d=4$ fm.

There exist the closely spaced doublet at 2.80 Mev excitations in ^{21}Ne. One state at 2.797 Mev is known to have $J^\pi=1/2^+$ from the (d, p) reaction.[34b] The other state at 2.791 Mev is suggested to be $J^\pi=3/2^+$ from the γ-γ and n-γ angular correlations.[34c] As seen from Fig. 7, the energies of this doublet are not reproduced sufficiently well in the present analysis without the intrinsic $(2s, 0)$ and $(1d, 0)$ configurations. The stripping pattern[34b] from 2.80 Mev excitations shows that the reaction takes place by a capture of a nucleon with zero angular momentum ($l=0$). Thus, in order to clarify the character of this doublet, it is necessary to describe completely the excited band with $\Omega=1/2$ in terms of the full configurations.

It has been found that reasonable agreement with the observed spectrum of the ground band can always be obtained when the potential parameters are taken to close to that of the phenomenological p-state N-α potential[10] and the state-dependent factor ξ is properly taken into account.

6. 3) *Ground state moments and electromagnetic transitions*

We can easily obtain the electromagnetic operators for the $\alpha+^{16}$O+ neutron system, by treating the former two particles as the structureless charged boson.

The magnetic dipole ($M1$) operator is given by

$$M(1, q) = \sqrt{3/4\pi}\, \mu_q , \tag{6·7}$$

where μ_q is the spherical component of the magnetic moment operator

$$\boldsymbol{\mu} = \mu_0 \{(1/2)\boldsymbol{J} + (g_n - 1/2)\boldsymbol{s}\} , \tag{6·8}$$

$\boldsymbol{J}$ being the total spin of ^{21}Ne, g_n the gyromagnetic ratio of a neutron and $\mu_0 = (e\hbar/2Mc)$. The electric quadrupole ($E2$) operator is given by Eq. (4·5), when we ignore the small corrections arising from the cranking effects of the centre-of-mass.

The magnetic dipole and electric quadrupole moments, μ and Q for a state with the spin J are written as

$$\mu = \mu_0 \{(J/2) + (g_n - 1/2)\,(2J+1)^{-1/2} (J1J0|JJ) \langle J \| s^{(1)} \| J \rangle\}, \tag{6·9}$$

$$Q = Q_0 (2J+1)^{-1/2} (J2J0|JJ) \langle J \| E^{(2)} \| J \rangle , \tag{6·10}$$

where the reduced matrix elements are defined in the Wigner-Eckart theorem[24] and Q_0 is the intrinsic Q-moment for the ^{20}Ne ($\alpha + ^{16}O$) core, i.e.

$$Q_0 = (16/5)\, e\, (\chi | R^2 | \chi) = (16/5)\, e d^2 . \tag{6·11}$$

The reduced transition probabilities for the $M1$ and $E2$ radiations, $B(M1; J \to J')$ and $B(E2; J \to J')$, from an initial state with the spin J to a final one with J' are given by

$$B(M1; J \to J') = (3/4\pi)\, \mu_0^2 (g_n - 1/2)^2 (2J+1)^{-1} |\langle J' \| s^{(1)} \| J \rangle|^2, \tag{6·12}$$

$$B(E2; J \to J') = (5/16\pi)\, Q_0^2 (2J+1)^{-1} |\langle J' \| E^{(2)} \| J \rangle|^2 . \tag{6·13}$$

For the states represented by Eq. (6·5) the reduced matrix elements are calculated with the standard method of the rotational model.[20]

Table III. The ground state μ and Q moments and the reduced $M1$ and $E2$ transition probabilities within the ground band in ^{21}Ne. The calculated values are obtained in terms of the wave functions listed in Table II.

(a) The ground state μ and Q moments.

	Cal	Exp [35]
μ(*n. m.*)	−0.748	−0.66
Q($e$fm^2)	9.94	9.3

(b) The reduced $M1$ transition probabilities.

J	J'	$B(M1, J \to J')$ (μ_0^2)	
		Cal	Exp [35]
$5/2^+$	$3/2^+$	0.168	$0.020^{+0.130}_{-0.011}$
$7/2^+$	$5/2^+$	0.125	$0.12^{+0.27}_{-0.06}$
$9/2^+$	$7/2^+$	0.139	$0.26^{+0.45}_{-0.16}$

(c) The reduced $E2$ transition probabilities.

J	J'	$B(E2; J \to J')$ (e^2 fm^4)	
		Cal	Exp [35]
$5/2^+$	$3/2^+$	78.1	150
$7/2^+$	$5/2^+$	55.3	19^{+60}_{-12}
$7/2^+$	$3/2^+$	32.8	20^{+39}_{-10}
$9/2^+$	$7/2^+$	38.3	41^{+18}_{-32}
$9/2^+$	$5/2^+$	52.6	22^{+38}_{-13}

The ground state μ and Q moments and the various $M1$ and $E2$ transition rates within the ground band are calculated in terms of the corresponding wave functions listed in Table II. The results are summarized in Table III and compared with the experimental data [34a,b),35)] in ^{21}Ne. Agreements are rather satisfactory.

The transitions from the doublet at the 2.80 Mev excitations to the members of the ground band have been observed experimentally.[34c,d)] These transitions are not investigated in this paper, because the excited bands with $\Omega=1/2$ are described incompletely in the present analysis, as mentioned in the previous subsection.

§ 7. The excited $K^\pi=2^-$ rotational band in ^{20}Ne

Motion of a particle-hole pair

7. 1) *State vectors and energy matrices*

In the two previous sections we have treated the three-body problems, i.e. the $\alpha+^{16}\mathrm{O}+h$ or p system, and have seen how the particle or hole motions are described. The next problem is to analyze the four-body one, i.e. the $\alpha+^{16}\mathrm{O}+p+h$ system. As an application, we will pick out the second Litherland band[25)] in ^{20}Ne, which starts from the 4.97 Mev excitation with $J^\pi=2^-, 3^-, \cdots$. This band has been interpreted as the $K^\pi=2^-$ octupole g-vibrational band.[25)] Experimental studies[36)] has suggested the $p^{-1}(sd)^5$ configuration for this band. Theoretical works[27),37)] have been done in terms of the method of deformed orbitals and the SU_3 model, on the basis of this configuration.

In the present model it is assumed that this band originates from the coupled motion of the α-cluster and a particle-hole pair. In the most energetically favourable configuration, a hole and a particle move on the spherical $p_{1/2}$-shell orbital and the deformed intrinsic one with $\Omega_p=3/2$ in the sd shell, respectively. In the relevant states the h-α interaction is weak as compared with the p-α and p-h ones (e.g. $-\langle V_{h\alpha}\rangle\cong 1$ Mev and $\langle V_{p\alpha}\rangle\cong-\langle V_{ph}\rangle\cong-3$ Mev). Therefore it may be expected that the motion of the hole correlates with that of the particle so as to make Ω a good quantum number approximately, where Ω $(=\Omega_p+\Omega_h)$ is the projection of the total angular momentum $\boldsymbol{j}$ $(=\boldsymbol{j}_p+\boldsymbol{j}_h)$ on the symmetry axis of the ^{20}Ne $(\alpha+^{16}\mathrm{O})$ core. Then, the states of the $\alpha+^{16}\mathrm{O}+h+p$ system can be described in terms of the strong-coupling bases in which the particle is specified with the $(l\Lambda)$ representation while the hole with the $(j\Omega)$ one. However, for simplicity, we will assume that the deformed intrinsic orbital of the particle with $\Omega_p=3/2$ can be approximated by means of the intrinsic state with $(j\Omega)_p=(1d_{5/2}, 3/2)$.

In this case the state vector with the definite total spin J, parity Π and isospin T is approximately represented as

$$|B;\ JM\rangle\equiv|p,\ h^{-1};\ JTMK=\Omega,\ \Pi=\pm\rangle=\sqrt{(2J+1)/16\pi^2}\chi(R)$$
$$\times\{D^J_{MK}(\Theta_i)\,[\alpha_p{}^+\times\beta_h{}^+]_T\pm(-)^\omega D^J_{M-K}(\Theta_i)\,[\alpha_{-p}{}^+\times\beta_{-h}{}^+]_T\}\,|\phi_0\rangle\,, \qquad (7\cdot1)$$

with $p\ (h)=\lambda_p\ (\lambda_h)$, $\lambda=(nlj,\ \Omega\tau)$ and $\omega=l_p+l_h+j_p+j_h+J$. Here, the meaning of each part and the notation involved are almost the same as those of the basic vector (6·1). The difference is the appearance of the hole operator $\beta_\lambda{}^+$, together with the particle one $\alpha_\lambda{}^+$. They are specified by the intrinsic states with $(j\Omega)_p=(1d_{5/2},\ \pm3/2)$ and $(j\Omega)_h=(1p_{1/2},\ \pm1/2)$, respectively. Note that the former state does not contain the orbit with $\Lambda_p=0$ which is strongly influenced by the s-state N-α repulsion. Furthermore, in the $(p_{1/2})^{-1}d_{5/2}$ configuration we are entirely free from the troublesome problem of the spurious excitation for the centre-of-mass motion of the ^{16}O core.[38]

The state vector (7·1) can be expressed in the space-fixed frame in terms of various transformations. We give here one of them which becomes necessary later:

$$|B;\ JM\rangle=\sum_{LJ_1}C_{SB}|S;\ JM\rangle \qquad (7\cdot2)$$

with the definitions

$$C_{SB}\equiv C^J_{JJ_1}(j_pj_h\Omega_p\Omega_h,\ \Pi=\pm)=[1\pm(-)^{l_p+l_h+L}]/\sqrt{2}$$
$$\times(-)^{J+L+\Omega}(Jj_h\Omega-\Omega_h|J_1\Omega_p)\,(J_1j_p\Omega_p-\Omega_p|L0)\,, \qquad (7\cdot3)$$
$$|S;\ JM\rangle\equiv|\,(Lp)J_1,\ h^{-1};\ JTM\rangle=\chi(R)$$
$$\times[[Y_L(\hat{\boldsymbol{R}})\times a_p{}^+]_{J_1}\times b_h{}^+]_{JTM}|\phi_0\rangle\,. \qquad (7\cdot4)$$

The matrix elements of the total Hamiltonian (2·1) between the state vectors (7·1) with $T=0$ can be written as

$$\langle B;\ JM|H|B';\ JM\rangle=-\sum_{J_1}(-)^{w(\Omega)}(Jj_h\Omega-\Omega_h|J_1\Omega_p)$$
$$\times(Jj_h\Omega'-\Omega_h'|J_1\Omega_p')\langle B;\ J_1M_1|H|B';\ J_1M_1\rangle_{\rm AV}\delta(j_h,j_h')$$
$$-(1/2)[(-)^{w(l)}+(-)^{w(j)}](h|\overline{V}_{N\alpha}|h')_{b,\,R=d,\,\rm AV}\delta(p,p')$$
$$-\varepsilon_{j_h,\,\rm AV}\delta(ph,p'h')-\sum_I(j_pj_h\Omega_p\Omega_h|I\Omega)\,(j_p'j_h'\Omega_p'\Omega_h'|I\Omega)$$
$$\times(ph^{-1};\ IT|v_{ph}|p'h'^{-1};\ IT)\,\delta(\Omega,\Omega')\,, \qquad (7\cdot5)$$

where $w(\lambda)=\lambda_h-\lambda_h'$ and the suffix AV denotes an average over the change states. The first term in Eq. (7·5) is derived by means of the transformation (7·2), where the state vector $|B;\ J_1M_1\rangle\equiv|p;\ J_1M_1\Omega_p\Pi_1=(-)^{l_p}\Pi\rangle$ is referred to the $\alpha+^{16}O+p$ system and is defined in a way similar to that in the case of the basic vector (6·1).

In evaluating the matrix elements (7·5), we assume that the state vectors $|B;\ J_1M_1\rangle$ with $(j\Omega)_p=(1d_{5/2},\ 3/2)$ can be regarded approximately as the eigenvectors for the members of the ground band in ^{21}Ne and ^{21}Na;

$$\{H-E_1(J_1)+\text{B.E.}(A=21)\}|B;J_1M_1\rangle\cong 0\,, \qquad (7\cdot6)$$

where $E_1(J_1)$ denotes the corresponding excitation energy. The validity of this approximation has been shown in § 6. The last term in Eq. (7·5) contains the p-h matrix elements which can be expressed in terms of the p-p ones, following to the standard manner.[39]

7. 2) *Energy spectra and electric transitions*

For the $(1p_{1/2}, \pm 1/2)^{-1}(1d_{5/2}, 3/2)$ configuration we have two rotational bands with $K=\Omega=1$ and 2 from the diagonal elements of Eq. (7·5). The energy spectra without the K band mixing are obtained only in the first order approximation, because of the simplified treatments for the state vector (7·1). In the calculations we use the experimental values for the excitation energies $E_1(J_1)$ and the h-α interaction energy $(1p_{1/2}, 1/2|\overline{V}_{N\alpha}|1p_{1/2}, 1/2)_b$. As the residual force

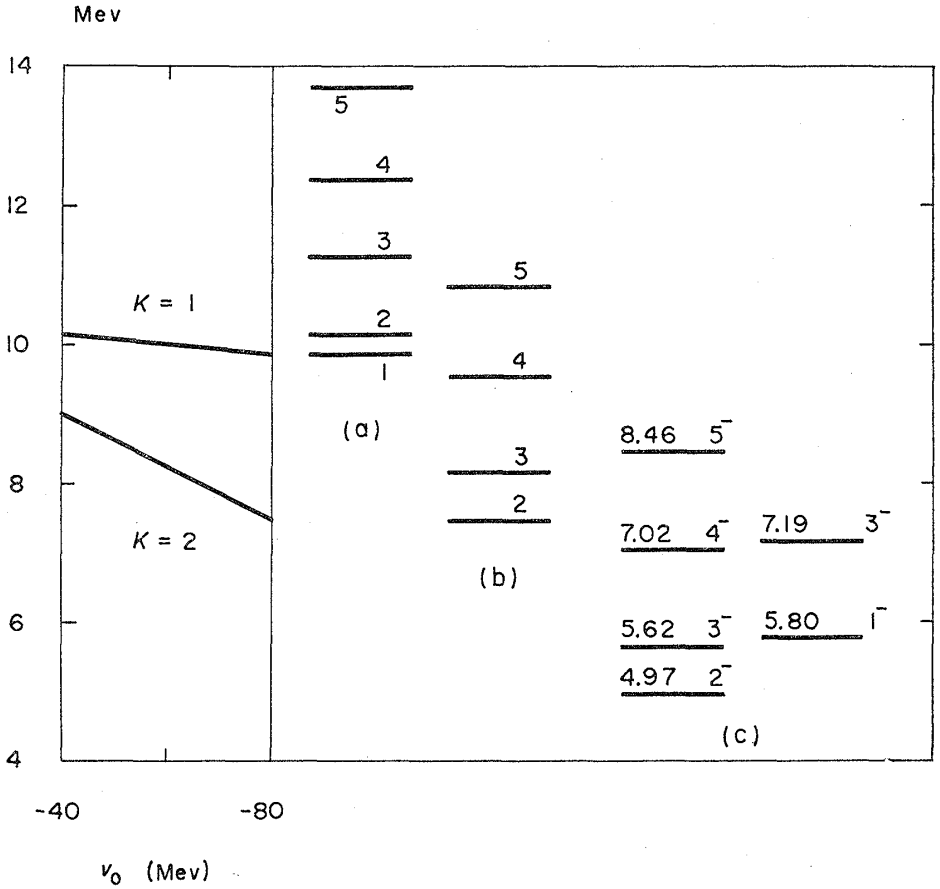

Fig. 8. Negative parity levels of ^{20}Ne, given relative to the observed binding energy of the 0^+ ground state. (a) and (b) indicate the rotational bands with $K^\pi=1^-$ and 2^-, respectively, based on the $(p_{1/2}, \Omega=1/2)^{-1}$ $(d_{5/2}, \Omega=3/2)$ configuration. (c) Experimental spectra. The particle-hole interaction energies are calculated in terms of the Yukawa force with the range $r_0=1.37$ fm and the Rosnfeld mixture and of the oscillator functions with the size parameter $b=1.64$ fm. On the left-hand of the figure, the band-head energies are plotted against v_0, the strength of the force.

between the nucleons we choose the Yukawa type with the Rosenfeld mixture and the range $r_0=1.37$ fm. The p-p matrix elements for this force is obtained in the usual way[22] in terms of the value $b=1.64$ fm, the size parameter of the harmonic oscillator functions. The calculated energy spectra are shown as a function of the strength v_0 of the residual force in Fig. 8, together with the experimental data.[25] The energies are given relative to the observed energy of the 0^+ ground state in ^{20}Ne.

Table IV. The reduced $E2$ transition probabilities within the $K^\pi=2^-$ rotational band in ^{20}Ne. The calculated values are based on the intrinsic Q moment determined with the α-^{16}O rms distance $d=4$ fm.

J	J'	$B(E2; J\to J')$ (e^2 fm^4)	
		Cal	Exp[40]
4^-	3^-	69.6	115
4^-	2^-	31.0	35.6

For the system treated the $E2$ operator is also given by Eq. (4·5), the effects of the single-particle transitions being ignored. Then, the reduced $E2$ transition probabilities within a K band are given by the well-known formula[20]

$$B(E2; JK\to J'K) = (5/16\pi)Q_0^2(J2K0|J'K)^2, \qquad (7\cdot7)$$

where Q_0 is defined in Eq. (6·11). The calculated values for the $K=2$ band are shown in Table IV in comparison with the experimental data,[40] where Q_0 is estimated with the value $d=4$ fm.

As seen from Fig. 8 and Table IV, the energy spectrum and $E2$ transitions are well accounted for in the $K^\pi=2^-$ band. However, the present model also predicts the $K^\pi=1^-$ band which is not observed experimentally at low excitaion energies.

The enhanced $E3$ transition has been observed between the 3^- level at 5.63 Mev and the 0^+ ground state in ^{20}Ne. The reduced $E3$ transition probability is estimated as $B(E3; 3^-\to0^+)_{exp}\cong1.8\times10^2e^2$ fm^6 from the observed enhancement factor[41] 7 over the single-particle estimate. However, the state (7·1) with $J^\pi=3^-$, $K=2$ representing the 3^- level at 5.63 Mev, because of its $1p$-$1h$ character, is connected with the 0^+ ground state (the $0p$-$0h$ state) only by single-particle $E3$ transitions. A possible explanation for the enhanced $E3$ transition is given by taking into account the effect of the mixing between the 3^- level at 5.63 Mev and the other 3^- level at 7.17 Mev. The latter level is considered as the state based on the α-^{16}O relative motion with $L=3$, as discussed in § 4. This 3^-, $K=0$ state indicates a collective $E3$ transition*) to the 0^+ ground state and can mix with the 3^-, $K=2$ state (7·1) by the coupling term H_I of Eq. (2·5). Evidences of this mixing have been suggested experimentally. In the inelastic scattering of α particles on ^{20}Ne, both the 3^- states at 5.63 and 7.17 Mev are equally excited.[42] In the $^{16}O(^7Li, t)^{20}Ne$ reaction the excitation of the two 3^- states are also observed.[36a]

*) In this case the $E3$ operator is given by $E(3, q)=(24/25)eR^3Y_{3q}(\hat{\boldsymbol{R}})$. An estimate gives $B(E3; 3^-\to0^+)=1.2\times10^3$ e^2 fm^6 with $\sqrt[3]{\langle R^3\rangle}=5$ fm.

§ 8. Summary and conclusion

The aim of this paper was to examine a possibility of α-cluster structure in the low-energy states of the nuclei around ^{20}Ne. For this purpose an attempt has been made to describe their properties dynamically in terms of an α-cluster plus ^{16}O-core model with effective α-^{16}O and N-α potentials. The model has been developed in such a manner as treating the coupled system of the α-^{16}O relative motion with the particle and hole ones in an average field of ^{16}O.

The main results are summarized as follows.

(I) The $K^\pi=0^+$ rotational band in ^{20}Ne ($\alpha+^{16}$O) can be described by effective α-^{16}O potentials having a repulsive core and a state-dependent well. Such potentials can give a plausible explanation for the deviations of the energy spectrum and $E2$ transitions from the rotational model. The energy gap between the $K^\pi=0^+$ and 0^- bands in ^{20}Ne is attributed to the systematic differences assumed for these potentials between the even and odd parity states.

(II) Both the low-lying anomalous-parity levels of ^{19}F ($\alpha+^{16}$O$+h$) and the ground rotational band in ^{21}Ne ($\alpha+^{16}$O$+p$) are reasonably understood in terms of an effective N-α potential which has the essential character of the N-α interaction in free space. Its s-state repulsion plays important roles in both systems: it brings on the appearance of the anomalous-parity states with low excitations in ^{19}F and also guarantees the consideration of the effects of the Pauli principle for the states of the ground band in ^{21}Ne. The motions of the hole and the particle are described with the weak-coupling scheme and the strong-coupling one, respectively, where the hole takes spherical p orbitals and the particle moves on deformed sd ones compatible with the Pauli principle.

(III) The excited $K^\pi=2^-$ rotational band in ^{20}Ne ($\alpha+^{16}$O$+p+h$) is also well interpreted as originating from the coupled motion of the α-cluster and particle-hole pair around the ^{16}O core. The motions of both the particle and hole are described in terms of the strong-coupling scheme, because of the relatively strong particle-hole interactions. The hole (particle) orbital in this band is determined to be consistent with the corresponding one in ^{19}F (^{21}Ne).

The model stands on the picture of the *weak coupling* between the α-cluster and the ^{16}O core. Of course, the model exhibits several defects because of this drastic and limiting assumption. Nevertheless, the model succeeds in explaining the various nuclear properties reasonably, as summarized above.

The successes of this model lead to the conclusion that α-like four-body correlations seem to be very important in the nuclei around ^{20}Ne.

Acknowledgements

This work was performed as a part of the "Annual Research Project for the Four-Body Correlation in Light Nuclei" organized by the Research Institute for Fundamental Physics in 1967. The authors would like to express their

sincere thanks to Prof. A. Arima and Prof. T. Marumori for valuable suggestions. They also wish to express their thanks to Prof. H. Tanaka and Prof. R. Tamagaki for stimulating discussions. Thanks are also due to other members of the research project and of our laboratory for their kind interests. Two of the authors (J. H. and Y. A.) are indebted to Takeda Science Foundation for financial aid. The numerical calculations were carried out using the NEAC-2203G and CLOAP-2000 computers at Hokkaido University.

References

1) Y. Abe, S. Saito, O. Endō and J. Hiura, *Contribution No. 4. 16 to the International Conference on Nuclear Structure, Tokyo* (1967).
2) J. P. Eliott and A. M. Lane, Handbuch der Physik **39** (1957), 241.
3) J. P. Eliott, Proc. Roy. Soc. **A245** (1958), 128, 562.
4) I. Kelson, Phys. Rev. **132** (1963), 2189.
I. Kelson and C. A. Levinson, Phys. Rev. **134** (1964), B269.
5) G. C. Phillips and T. A. Tombrello, Nucl. Phys. **19** (1960), 555.
P. K. Sheline and K. Wildermuth, Nucl. Phys. **21** (1960), 196.
H. Tanaka, in *Proceedings of the International Conference on Nuclear Structure, Tokyo, 1967* (J. Phys. Soc. Japan, Suppl. **24** (1968), 51).
6) K. Wildermuth and W. McClure, *Cluster Representation of Nuclei* (Springer-Verlag, Berlin, 1966).
Yu. A. Kudeyarov, Z. Matthies, V. G. Neudachin and Yu. F. Smirnov, Nucl. Phys. **65** (1965), 529.
S. Saito, J. Hiura and H. Tanaka, Prog. Theor. Phys. **39** (1968), 635.
7) J. Hiura and I. Shimodaya, Prog. Theor. Phys. **30** (1963), 585; **36** (1966), 977.
8) a) H. Kanada, S. Nagata, S. Otsuki and Y. Sumi, Prog. Theor. Phys. **30** (1963), 475.
b) R. E. Schenter, Nucl. Phys. **A94** (1967), 408; Phys. Rev. Letters **18** (1967), 465.
9) I. Shimodaya, R. Tamagaki and H. Tanaka, Prog. Theor. Phys. **27** (1962), 793.
R. Tamagaki and H. Tanaka, Prog. Theor. Phys. **34** (1965), 191.
S. Okai and S. C. Park, Phys. Rev. **145** (1966), 787.
R. Tamagaki, Prog. Theor. Phys. Suppl. Extra Number (1968), 242.
S. Saitō, Prog. Theor. Phys. **40** (1968), 893; **41** (1969), 705.
10) a) S. Sack, L. C. Biedenharn and G. Briet, Phys. Rev. **93** (1954), 321.
b) P. Swan, Phys. Rev. Letters **19** (1967), 245.
11) O. Endō, I. Shimodaya and J. Hiura, Prog. Theor. Phys. **31** (1964), 1157.
P. Darriulat, G. Igo, H. G. Pugh and H. D. Holmgren, Phys. Rev. **137** (1965), B315.
12) A. Arima, H. Horiuchi and T. Sebe, Phys. Letters **24B** (1967), 129.
T. Engeland and P. J. Ellis, Phys. Letters **25B** (1967), 57.
13) T. Marumori and K. Suzuki, Nucl. Phys. **A106** (1968), 610.
14) J. Eichler, T. Marumori and K. Takada, Prog. Theor. Phys. **40** (1968), 60.
15) H. Horiuchi and K. Ikeda, Prog. Theor. Phys. **40** (1968), 277.
16) A. Bohr and B. R. Mottelson, Kgl. Danske Videnskab. Selskab, Mat.-fys. Medd. **27** (1953), No. 16.
17) S. S. Schweber, H. A. Bethe and F. de Hoffmann, *Mesons and Fields* (Row, Peterson and Company, Evanston, 1955), Vol. I, p. 203.
18) E. U. Condon and G. H. Shortly, *The Theory of Atomic Spectra* (Cambridge University Press, London, 1935).
19) G. E. Brown, *Unified Theory of Nuclear Models* (North-Holland Publishing Company, Amsterdum, 1964).
20) S. A. Moszkowski, Handbuch der Physik **39** (1957), 410.

21) S. G. Nilsson, Kgl. Danske Videnskab. Selskab, Mat.-fys. Medd. **29** (1955), No. 16.
22) A. de-Shalit and I. Talmi, *Nuclear Shell Theory* (Academic Press, New York and London, 1963).
23) L. R. B. Elton, *Nuclear Sizes* (Oxford University Press, 1961).
24) U. Fano and G. Racah, *Irreducible Tensorial Sets* (Academic Press Inc., New York, 1959).
25) A. E. Litherland, J. A. Kuehner, H. E. Gove, M. A. Clark and E. Almqvist, Phys. Rev. Letters **7** (1961), 98.
J. A. Kuehner and E. Almqvist, Can. J. Phys. **45** (1967), 1605.
26) T. Inoue, T. Sebe, H. Hagiwara and A. Arima, Nucl. Phys. **59** (1964), 1.
A. Arima, S. Cohen, R. D. Lawson and M. H. Macfarlane, Nucl. Phys. **A108** (1968), 94.
J. Flores and R. Perez, Phys. Letters **26B** (1967), 55.
27) J. P. Eliott, in *Selected Topics in Nuclear Theory*. ed. S. Eklund (International Atomic Energy Agency, Vienna, 1963).
W. H. Bassichis, C. A. Levinson and I. Kelson, Phys. Rev. **136** (1964), B380.
28) H. C. Evans, M. A. Eswaran, H. E. Gove, A. E. Litherland and C. Broude, Can. J. Phys. **43** (1965), 82.
29) E. B. Paul, Phil. Mag. **15** (1957), 311.
M. Harvey, Nucl. Phys. **52** (1964), 542.
W. H. Bassichis, B. Girand and G. Ripka, Phys. Rev. Letters **15** (1965), 980.
30) M. Baranger, Phys. Rev. **120** (1960), 957.
31) J. D. Prentice, N. W. Gebbie and H. F. Caplan, Phys. Letters **3** (1963), 201.
A. E. Litherland, M. A. Clark and C. Broude, Phys. Letters **3** (1963), 204.
32) G. J. Wagner and P. J. Ellis, Phys. Letters **26B** (1968), 429.
33) J. M. Freeman, Phys. Rev. **120** (1960), 1436.
B. E. Chi and J. P. Davidson, Phys. Rev. **131** (1963), 366.
R. M. Dreizler, Phys. Rev. **132** (1963), 1166.
34)a) R. D. Bent, J. E. Evans, G. C. Morrison, N. H. Gale and I. J. van Heerden, Nucl. Phys. **A90** (1967), 122.
b) A. J. Howard, J. P. Allen, D. A. Bromley, J. W. Olness and E. K. Warburton, Phys. Rev. **157** (1967), 1022.
c) P. J. M. Smulders and T. K. Alexander, Phys. Letters **21** (1966), 664.
d) J. G. Pronko, C. Rolfs and H. J. Mair, Nucl. Phys. **A94** (1967), 561.
35)a) J. T. La Tourrette, W. E. Quinn and N. F. Ramsey, Phys. Rev. **107** (1956), 1202.
b) G. M. Grosof, P. Buck, W. Lichten and I. I. Rabi, Phys. Rev. Letters **1** (1958), 214.
c) S. J. Skorka, J. Hertel and T. W. Retz-Schmidt, *Nuclear Data* (Academic Press, New York and London), **A2** (1966), 347.
36)a) R. H. Siemssen, R. Felst, M. Cosack and J. L. Weil, Nucl. Phys. **52** (1964), 273.
b) R. H. Siemssen, L. L. Lee, Jr. and D. Cline, Phys. Rev. **140** (1965), B1258.
c) R. Middleton, B. Rosner, D. J. Pullen and L. Polsky, Phys. Rev. Letters **20** (1968), 118.
37) C. J. Borse and J. M. Eisenberg, Phys. Letters **22** (1966), 630.
38) E. Baranger and C. W. Lee, Nucl. Phys. **21** (1961), 157.
39) A. Kallio and K. Kolltveit, Nucl. Phys. **53** (1964), 87.
40) C. Broude, M. A. Clark and A. E. Litherland, Phys. Letters **3** (1962), 118.
41) C. Broude, A. E. Litherland and J. D. Pearson, Phys. Letters **11** (1964), 321.
42) A. Springer and B. G. Harvey, Phys. Rev. Letters **14** (1965), 316.